

***In Vivo* Low-level Light Therapy Increases Cytochrome Oxidase in Skeletal Muscle**

Christopher R. Hayworth^{1,2}, Julio C. Rojas¹, Eimeira Padilla¹, Genevieve M. Holmes¹, Eva C. Sheridan¹ and F. Gonzalez-Lima^{*1}

¹Departments of Psychology, Pharmacology and Toxicology, Institute for Neuroscience, University of Texas at Austin, Austin, TX

²Department of Neuroscience, School of Medicine, University of Pennsylvania, Philadelphia, PA

Received 15 January 2010, accepted 23 February 2010, DOI: 10.1111/j.1751-1097.2010.00732.x

ABSTRACT

Low-level light therapy (LLLT) increases survival of cultured cells, improves behavioral recovery from neurodegeneration and speeds wound healing. These beneficial effects are thought to be mediated by upregulation of mitochondrial proteins, especially the respiratory enzyme cytochrome oxidase. However, the effects of *in vivo* LLLT on cytochrome oxidase in intact skeletal muscle have not been previously investigated. We used a sensitive method for enzyme histochemistry of cytochrome oxidase to examine the rat temporalis muscle 24 h after *in vivo* LLLT. The findings showed for the first time that *in vivo* LLLT induced a dose- and fiber type-dependent increase in cytochrome oxidase in muscle fibers. LLLT was particularly effective at enhancing the aerobic capacity of intermediate and red fibers. The findings suggest that LLLT may enhance the oxidative energy metabolic capacity of different types of muscle fibers, and that LLLT may be used to enhance the aerobic potential of skeletal muscle.

INTRODUCTION

Cytochrome oxidase is a key molecule for aerobic life. It is the most abundant mitochondrial heme-containing metalloprotein and plays a central regulatory role in energy metabolism. Cytochrome oxidase, or complex IV, is the terminal protein complex of the electron transport chain and catalyzes the reduction of more than 90% of the oxygen taken up by aerobic organisms (1). It constitutes an efficient energy transducer device, acting as a redox-linked proton pump that contributes to the transmembrane electrochemical gradient and as a rate-limiting step for the synthesis of the energy-storing molecule adenosine triphosphate (ATP) (2–5). Because its activity and induction are tightly coupled to metabolic demands (6), plasticity (7), cell survival signaling and calcium metabolism (8,9), cytochrome oxidase is a crucial mediator of cellular homeostasis. Moreover, the catalytic activity of cytochrome oxidase is routinely used to define the oxidative potential of muscle fibers, and as a reliable quantitative marker of cellular metabolic capacity, especially in tissues with high energy demands like skeletal muscle and brain (10,11). Cytochrome

oxidase is also a well-established primary photoacceptor of light in the red to near-infrared region of the visible spectrum in animal tissues, and has been implicated in the mechanism of action of developing photobiomodulation technologies (12–16).

Low-level light therapy (LLLT) has been shown to influence a wide variety of cellular functions, including gene expression (17,18), growth and proliferation (19) and survival (20,21). We have previously shown that LLLT is effective at preventing neurodegeneration in a model of mitochondrial optic neuropathy (22). Skeletal muscle, a tissue with a high rate of aerobic energy metabolism, is highly susceptible to the stimulatory effects of LLLT. In skeletal muscle, LLLT has been effective at promoting improvements in electrical activity (23), preventing fatigue induced by tetanic contractions (24), improving healing after traumatic injury (25–27) and preventing snake venom-induced rhabdomyolysis (28). A central hypothesis of the mechanism underlying these beneficial effects is that LLLT directly stimulates the activity of cytochrome oxidase in muscle fibers, triggering a series of biochemical cascades that improve cellular functions (15). In tissues other than muscle, this cascade of events has been demonstrated to include increased enzymatic activity of the mitochondrial respiratory complexes (29), upregulation of cytochrome oxidase activity (30), enhancement of oxygen consumption (22) and increased ATP concentration (31). Recently, Silveira *et al.* (32) demonstrated that, in skeletal muscle, LLLT facilitated the enhancement in mitochondrial enzymatic activity following traumatic muscle injury, but there is no previous description of the *in vivo* effects of LLLT on the cytochrome oxidase activity of intact skeletal muscle. The present study tested the hypothesis that *in vivo* LLLT, delivered in a single fraction with light-emitting diode arrays, enhances the cytochrome oxidase activity of skeletal muscle fibers, as measured by a histochemical method highly sensitive to quantitative changes in cytochrome oxidase activity.

MATERIALS AND METHODS

Subjects. Holtzman rats ($n = 40$, 19 males, 21 females, 570 g) were initially obtained from Harlan (Madison, WI) and then bred in a colony in the Animal Resources Center at the University of Texas at Austin. Subjects were handled regularly after weaning, maintained in clear plastic cages with food and water *ad libitum* and subjected to

*Corresponding author email: gonzalez-lima@mail.utexas.edu (F. Gonzalez-Lima)

© 2010 The Authors. Journal Compilation. The American Society of Photobiology 0031-8655/10

standard light cycles (12 h light/12 h dark) before and after treatments. All possible measures were taken to minimize animal distress. All experimental procedures were approved by the Institutional Animal Care and Use Committee of the University of Texas at Austin. Unless otherwise specified, all chemical reagents were purchased from Sigma-Aldrich (St. Louis, MO).

Low-level light therapy delivery. Low-level light therapy was delivered *via* narrow-angle GaAlAs light-emitting diodes (LED) (peak $\lambda = 660$ nm, spectral line half-width $\Delta\lambda = 21$ nm, viewing angle = 20°) purchased from LEDtronics, Inc. (Torrance, CA) and assembled in our laboratory on fiberglass circuit boards to build 5.5×9.5 cm arrays (Fig. 1A). A 1Ω resistor and an AC 100 V, 0.8 A, 50–60 Hz power supply were used for each array, which contained 149 LED. Four arrays were mounted on a cardboard cage lid and they were 4 cm above the subjects' heads. With this setup, the light source produced negligible amounts of surface heat and induced a temperature change $< 1^\circ\text{C}$ over 10 min at 4 cm. Each array irradiated one quadrant of the animal cage with an irradiance of 9 mW cm^{-2} , as determined by means of a Newport 1830C power meter (Newport, Irvine, CA). This irradiance was chosen based on preliminary studies showing that low irradiances ($< 10 \text{ mW cm}^{-2}$) are able to stimulate brain cytochrome oxidase *in vivo* with relatively short exposure times to living rats, thus preventing significant behavioral disruption. A dose–response curve was attempted with cumulative doses of 20 J cm^{-2} , which have resulted in cytochrome oxidase stimulation in previous studies (20,22,31). Thus, LLLT was delivered with a noncontact modality to subjects in their cages (two to three subjects per cage, all same sex), in a dark room, and in a single session of either 20, 40 or 60 min for total doses of 10.8 J cm^{-2} (LLLT 1, $n = 10$, 5 males, 5 females), 21.6 J cm^{-2} (LLLT 2, $n = 9$, 4 males, 5 females) and 32.4 J cm^{-2} (LLLT 3, $n = 10$, 5 males, 5 females). Subjects in the control group ($n = 11$, 5 males, 6 females) were housed in the dark for

20 min, but received no LLLT. Twenty-four hours after the LLLT session, animals were euthanized by decapitation to avoid any interference of anesthetic or sedative agents with the histochemical properties of the tissue. The temporalis fossae were exposed and bilateral and complete dissection of the temporalis muscle was performed. This skeletal muscle was selected for being the largest and most accessible to LLLT with our delivery apparatus and for being easily dissectible. In addition, the temporalis muscle was selected because of its relatively heterogeneous muscle fiber type composition (Fig. 1B), with at least two distinct zones: a superficial zone composed mainly of *white fibers* (*i.e.* fast-twitch, fatigable, glycolytic, type IIB, Fig. 1C) and a lower proportion of *intermediate fibers* (*i.e.* fast-twitch, fatigue-resistant, type IIA, Fig. 1D), and a deep zone, composed mainly of *red fibers* (*i.e.* slow-twitch, fatigue-resistant, type I, Fig. 1E) (33,34). Specimens were frozen in liquid nitrogen-cooled isopentane at -40°C . Serial $40 \mu\text{m}$ -thick transverse sections were obtained of the right temporalis muscle of each subject at -18°C using a Leica CM300 cryostat (Leica Microsystems, Bannockburn, IL). The plane of section was perpendicular to the main orientation of muscle fibers. Frozen sections were immediately mounted on glass slides to create three adjacent series for histochemical analysis. Slides were stored at -40°C until further use.

Cytochrome oxidase enzyme histochemistry. Temporalis muscle and tissue standard sections were stained with a cytochrome oxidase enzyme histochemistry procedure that shows a very high sensitivity to quantitative activity changes, as described previously (35,36). This histochemical method is also standard for identification of muscle fiber types with light microscopy (11). Frozen sections were prefixed in 0.5% glutaraldehyde/10% sucrose in phosphate buffer (PB), pH 7.6 for 5 min at 4°C , followed by three baths of 10% sucrose in PB (5 min each, allowing for gradual increases in temperature). The sections were incubated for 10 min in a solution containing 50 mM Tris, 1.1 mM

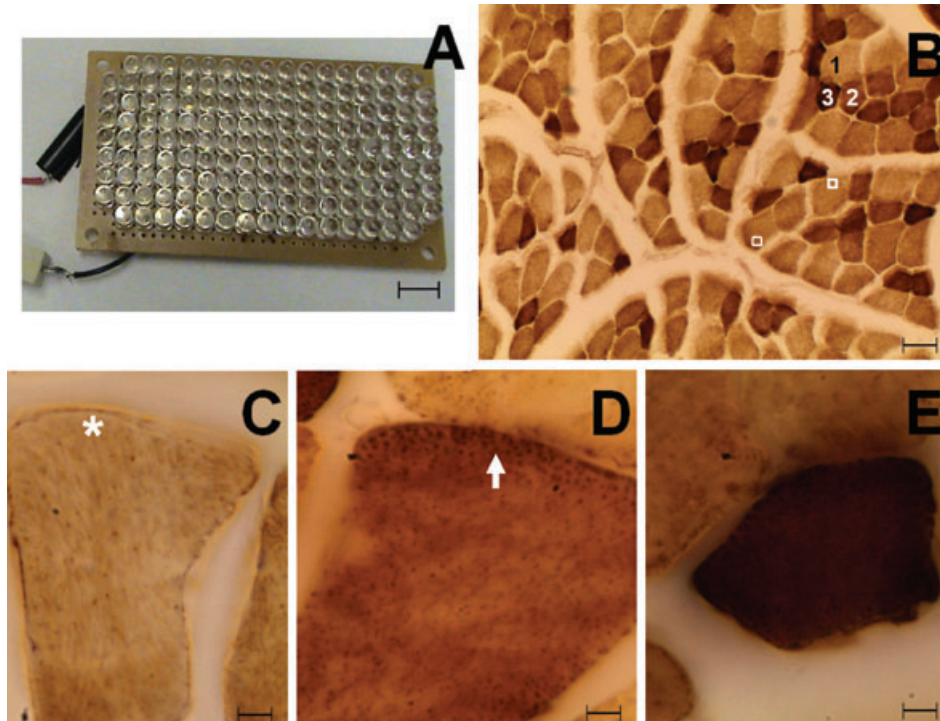


Figure 1. Light-emitting diode (LED) array and approach for quantification of cytochrome oxidase activity in the rat skeletal muscle. (A) Four GaAlAs LED arrays built on circuit boards like the one shown here were used to deliver low-level light therapy (LLLT) to rats *in vivo*. These arrays constituted an accessible, convenient and efficient way of delivering LLLT. Scale bar = 1 cm. (B) Fibers of different staining intensity levels (1–3) could be visualized in the superficial region of the temporalis muscle ($\times 200$). For quantifying optical density, sampling frames were systematically positioned over the darkest portion of the subsarcolemmal sarcoplasm of each fiber (white squares). (C) A higher power magnification ($\times 400$) of a white fiber shows scant cytochrome oxidase activity both at the center and periphery (asterisk) of the fiber. (D) In contrast, an intermediate muscle fiber demonstrates abundant mitochondria in their subsarcolemmal sarcoplasmic location (arrow). Mitochondria appear as multiple and discrete granules of intense chromophore precipitation at the fiber periphery. (E) A red fiber shows an intense homogeneous cytochrome oxidase staining. Scale bars (100, 20 and $5 \mu\text{m}$ in A, B and C–E, respectively).

cobalt chloride, 10% sucrose and 0.5% DMSO. After a 5 min rinse in PB at room temperature, the sections were stained for 60 min at 37°C in a PB solution containing 1.3 mM 3,3'-diaminobenzidine tetrahydrochloride, 75 mg L⁻¹ cytochrome *c*, 20 mg L⁻¹ catalase, 5% sucrose and 0.25% DMSO. Sections were fixed in 4% formalin in PB at room temperature for 30 min, dehydrated in series of 30–100% ethanol series, cleared in xylene (two times, 5 min each) and coverslipped with Permount®.

Muscle cytochrome oxidase activity quantification. Cytochrome oxidase activity was quantified by optical densitometry as detailed by Gonzalez-Lima and Cada and it was used as a marker of cell aerobic metabolic capacity (35,36). Optical density values of sampled muscle were converted to units of cytochrome oxidase activity using linear calibration curves based on standards of tissue thickness (10–80 μm thick) and spectrophotometrically determined cytochrome oxidase activity. Approaches for quantification of cytochrome oxidase activity were used to answer the following questions: (1) what is the dose–response effect of LLLT on muscle cytochrome oxidase activity? and (2) is there a differential effect of LLLT on each muscle fiber type? Accordingly, different approaches were implemented to quantify the effects of LLLT on muscle cytochrome oxidase activity. In the first approach, stained sections were placed on a DC-powered light box, digitized and analyzed using a CCD camera (Javelin Electronics, Torrance, CA), a Targa-M8 digitizer and JAVA imaging software (Jandel Scientific, Corte Madera, CA). Digitized images were corrected for slide and light box artifacts by means of background subtraction. Four samples spanning most of the specimen width were taken in each of the two temporalis muscle regions per subject (superficial and deep). A low-power view of the specimen allowed the identification of these two discrete zones. The median optical density value for each subject was obtained, transformed to cytochrome oxidase activity units and averaged to obtain mean group values. Cytochrome oxidase activity was reported as μmol min⁻¹ g⁻¹ of wet tissue. In the second approach, cross-sections of individual muscle fibers were analyzed one at a time at ×100 under a BX40 system microscope (Olympus America, Lake Success, NY) connected to the CCD camera and JAVA imaging software. The calibration and correction procedures used for the microscopic analysis of sections were similar to the one used in the first approach. All muscle fibers in view were sampled once adjacent to the cell membrane in order to obtain peak subsarcolemmal sarcoplasmic cytochrome oxidase activity values (Fig. 1C,D). Mean group values were expressed as optical density units. For display purposes, images were captured with a Leica DFC290 HD microscope camera mounted on a BX40 system microscope (Olympus America) and processed with Leica Application Suite software 1.5 (Leica Microsystems, Wetzlar, Germany).

Muscle thickness. An estimate of approximately 3 mm of superficial-to-deep thickness was obtained by a stereological distance measurement in the anterior portion of the superficial temporalis muscle that controlled for biases introduced by muscle shape (37). Temporalis muscle images of sections were digitized with a CCD camera (Javelin Electronics), and JAVA imaging software (Jandel Scientific). An isotropic uniform random system of test lines was superimposed on one sample per subject and distances between intercepts of each line with the superficial and deep borders of the muscle were measured. An unbiased estimate of temporalis muscle thickness was obtained as $T_{\text{temp}} = \Sigma \text{Length of intercept} / \text{No. of intercepts}$.

Statistical analysis. Multiple group comparisons were made with the Jonckheere-Terpstra independent samples nonparametric test, which accounted for the use of median optical density values and the directional order of groups intrinsic to the treatment design (*i.e.* increasing LLLT dosages) (38). Main effects, simple effects and interactions of LLLT dose, muscle depth and sex on the cytochrome oxidase activity values were determined with multivariate analysis of variance. To address whether group differences in cytochrome oxidase activity could be attributed to main weight or age differences between males and females, subject weight and age were used as covariates. For data obtained through microscopic inspection, optical density values were used in an exploratory data analysis protocol to determine normality and the presence of outlier values for each subject, which allowed assessing the presence of one or more muscle fiber populations. Values from individuals in each group were pooled to estimate the measures of central tendency and dispersion for that group. The

“pooled” standard deviation and mean values were used to determine the values comprised within 95% of the sampling distribution on an individual basis. Values falling outside this distribution were considered significantly different from those within it, which allowed classifying fibers in categorical populations based on their optical density values. The average values of the different populations were corroborated to be different by means of two-tailed, unequal variance, independent samples *t*-tests and a cross-validated canonical discriminant analysis. The discriminant analysis corroborated that with the approach presented above, three distinct fiber populations were effectively differentiated (Wilk's lambda = 0.238, $P < 0.001$). Moreover, 95% of white fibers, 100% of intermediate fibers and 88% of red fibers in both the control and treatment groups were correctly classified by the statistically based approaches. The influence of fiber type on LLLT effects was analyzed using two approaches: (1) comparing the mean optical density values of each fiber type between groups and (2) comparing the proportion of each fiber type present in the sample between treatment groups. The optical density means of each fiber type population and the muscle thickness were compared between groups with two-tailed, independent samples *t*-tests. Differences in the proportion of fibers between groups were computed with the chi-square or Fisher's exact test, when indicated, using control counts as expected values. All statistical tests were carried out using SPSS 11.0. $P < 0.05$ was considered significant.

RESULTS

Low-level light therapy enhanced muscle cytochrome oxidase activity in a hormetic dose–response fashion

To determine the dose–response effects of LLLT therapy on skeletal muscle oxidative metabolic capacity, rats were exposed to one of three LLLT doses, and temporalis muscles were removed and stained for cytochrome oxidase activity. Overall increased cytochrome oxidase activity in LLLT-treated groups was observed only in the superficial temporalis muscle. Of the three LLLT doses tested (LLLT 1, 2 and 3), the middle dose LLLT 2 (21.6 J cm⁻²) induced the largest increase (30%) in mean cytochrome oxidase activity compared with the untreated control ($112.4 \pm 11 \mu\text{mol min}^{-1} \text{g}^{-1}$ vs $86.2 \pm 4 \mu\text{mol min}^{-1} \text{g}^{-1}$, respectively, $P < 0.05$). In contrast, the lowest dose LLLT 1 (10.8 J cm⁻²) induced a 23% increase ($106.3 \pm 14 \mu\text{mol min}^{-1} \text{g}^{-1}$) whereas the highest dose group LLLT 3 (32.4 J cm⁻²) produced a mean cytochrome oxidase activity increase of only 8% ($93.4 \pm 7 \mu\text{mol min}^{-1} \text{g}^{-1}$) (Fig. 2A). Although LLLT induced a dose-dependent increase in metabolic capacity in the skeletal muscle, the observed effects do not fit the traditional linear threshold dose–response curve. Rather, the data suggest a dose–response curve typical of hormesis, whereby low and high doses produce cellular responses that are less robust compared to middle doses.

To determine if LLLT-induced increases in cytochrome oxidase activity observed in the temporalis muscle were dependent upon tissue thickness, a multivariate analysis including simple-effect tests was performed for each treatment group at 0.5 mm increments along the superficial-to-deep axis of the temporalis muscle. Overall, in the superficial region of the temporalis muscle, mean cytochrome oxidase activity steadily increased in a gradient-like fashion as a function of depth in all three treatment groups (LLLT 1, 2 and 3) and untreated control ($F_{(5,180)} = 16.8$, $P < 0.001$). Within the untreated control there was a slight baseline trend for a higher cytochrome oxidase activity in females than in males in both superficial (8%, $P = 0.46$) and deep (13%, $P = 0.08$) temporalis muscle regions. Significant sex × group interactions were observed only

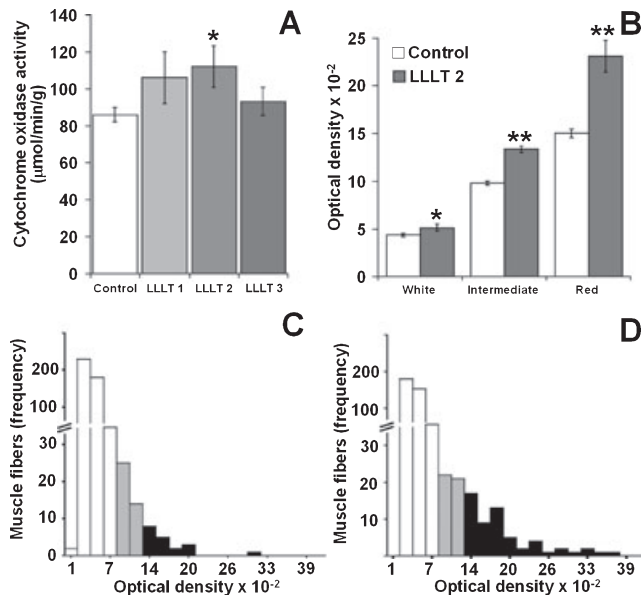


Figure 2. Effects of low-level light therapy (LLLT) on skeletal muscle cytochrome oxidase activity. (A) In the superficial temporalis muscle, LLLT induced increases in mean cytochrome oxidase activity in a dose–response manner. A middle dose (LLLT 2) was more effective than low (LLLT 1) and high (LLLT 3) doses. This dose–response curve is typically described as hormetic. (B) Superficial temporalis muscle fiber types display differential metabolic plasticity in response to LLLT. LLLT induced significant increases in mean cytochrome oxidase activity compared with the control, especially in red and intermediate fibers, whereas the induction of this enzyme was more subtle in white fibers. (C, D) The effects of LLLT were also evident as a change in the proportion of muscle fibers with low, intermediate and high cytochrome oxidase activity. The graphs depict frequency distributions of optical densities of individual superficial temporalis muscle fibers after cytochrome oxidase histochemistry. These represent pooled data from all subjects in the control (C) and LLLT 2 (D) groups. In both groups, the most abundant fiber type is white (low optical density, white bars). However, the distribution of LLLT 2-treated subjects has a higher range and frequency of fibers with higher optical density (black bars) than the control. Both distributions are polymodal, which suggests the presence of more than one fiber population. * $P < 0.05$, ** $P < 0.01$, compared with the control. LLLT 1 = 10.8 J cm^{-2} , LLLT 2 = 21.6 J cm^{-2} and LLLT 3 = 32.4 J cm^{-2} .

in the superficial temporalis muscle, which was thinner for females ($1.56 \pm 0.06 \text{ mm}$) compared with males ($1.88 \pm 0.09 \text{ mm}$) ($t_{(1,39)} = 2.7$, $P < 0.01$). In addition, there were significant sex differences in body weight (males = $699 \pm 12 \text{ g}$, females = $360 \pm 5 \text{ g}$, $t_{(1,32)} = 29$, $P < 0.001$). Therefore, smaller females with thinner muscles showed a greater response to the low-dose treatment. However, after covariance analysis of cytochrome oxidase activity accounting for body weight and muscle thickness, the differences remained between males and females.

LLLT induced a shift toward increased oxidative capacity in individual muscle fibers

In the untreated controls, microscopic examination of individual muscle fibers located in the superficial temporalis muscle revealed three discrete fiber populations based on cytochrome oxidase staining optical density values: white (light stain), intermediate (intermediate stain) and red (dark stain)

(Fig. 1). The vast majority of superficial temporalis muscle fibers were stained white (89%), with less frequent intermediate (7%) and very few red fibers (4%). Muscles of subjects treated with the effective LLLT dose (LLLT 2) were examined to determine the differential effects of LLLT as a function of muscle fiber type. The response of the three metabolic fiber types to LLLT-induced changes in cytochrome oxidase activity was verified by (1) comparing the mean optical density values of each fiber type between groups (Fig. 2B) and (2) comparing the frequency distribution of each fiber type present in the sample between treatment groups (Fig. 2C,D). Remarkably, LLLT 2 induced an increase in the mean optical density of the three fiber populations, but it was considerably higher in intermediate and red fibers. Compared with the control, white fibers in the LLLT 2 showed a mean cytochrome oxidase activity only 18% higher. Intermediate fibers in the LLLT 2 showed cytochrome oxidase activity levels 36% higher than control, whereas red fibers in the LLLT 2 group showed the highest change, with 54% more cytochrome oxidase activity compared with the control (Fig. 2B).

Regarding the effects of LLLT on fiber type composition, fibers in the LLLT 2 group (Fig. 2D) displayed a higher dispersion of optical density values, with increased frequencies of red fibers, compared with the control (Fig. 2C). These results were observed on an individual basis or when values in each group were pooled. Both the control and LLLT 2 groups showed positively skewed polymodal distributions, suggesting the presence of three metabolic muscle fiber classes. Whereas the proportion of white fibers did not change significantly after LLLT, the proportion of intermediate stained fibers in the LLLT 2 group was 68% less than expected, based on the control group count ($P < 0.05$). Similarly, the observed red fiber content in the LLLT 2 group tended to be at least twice as high as expected (Fig. 2D). Together, these data suggest that fibers with higher baseline oxidative potential are more amenable to metabolic potentiation with LLLT. In particular, the notable shift of intermediate stained fibers toward increased oxidative capacity upon LLLT stimulation indicates an exquisite metabolic plasticity in the intermediate fiber type.

DISCUSSION

Previous studies have shown that wavelengths of light at and around the near-infrared range can be delivered in doses too low to cause damage yet high enough to stimulate cellular activities including upregulated activity of photosensitive enzymes like cytochrome oxidase (18,19,22,30). This is the first report of a dose-dependent enhancement of cytochrome oxidase activity of skeletal muscle with *in vivo* LLLT that was detected at 24 h after treatment. Also, the quantitative fiber analysis in the superficial temporalis muscle demonstrated that intermediate and red fibers showed the strongest metabolic plasticity in response to treatment. LLLT-treated subjects showed a greater proportion of red fibers compared with the control, and the mean cytochrome oxidase activity of the remaining intermediate fibers (*i.e.* those statistically still categorized as intermediate) also showed remarkable increases in cytochrome oxidase activity after LLLT. Two aspects of the experimental design strengthen the internal validity of the findings. First, it is unlikely that the results were affected by systematic fiber classification bias. Fibers were statistically

classified with a high grade of accuracy. The misclassifications of red fibers reported in the discriminant analysis are due to the reduction in the sample size inherent in the cross-validation procedure. A reduction in the sample size was expected to increase the variance and the chance of error in this group in particular, due to the low frequency of red fibers. However, this misclassification affected data in both the control and experimental groups and it is conservative, as it occurred in a direction opposite to those of the effects expected with LLLT (*i.e.* 15% of red fibers were classified as intermediate fibers, as opposed to intermediate fibers being misclassified as red fibers). Further, the change in frequency of red fibers induced by LLLT was several orders of magnitude higher than the chance of red fiber misclassification. Also, rats were housed in a room receiving illumination from 32 W cool white fluorescent lamps with a color temperature of 4100 K, and a color rendering index of 62. With these parameters, the major luminous intensity peaks (2–3 mW) from this type of ambient light source occur at wavelengths around 440 and 540 nm, while comparatively negligible peaks are detected at 660 nm (39). In addition, the average illuminance within individual cages was only 116 lm m⁻² and subjects from all groups, including controls, were housed in the same conditions. For these reasons, it is unlikely that the effects of LLLT on muscle cytochrome oxidase were systematically biased by ambient light conditions.

LLLT has been proposed to stimulate tissue chromophores, inducing electronically excited states that modify their redox potential and catalytic activity. Such events are believed to subsequently activate a variety of intracellular signaling and metabolic pathways that modulate cellular functions (40). In this study, cytochrome oxidase was induced by LLLT, revealing a remarkable metabolic plasticity in muscle 24 h after a single stimulation treatment. These data implicate muscle fiber cytochrome oxidase as a potential mechanistic mediator of the beneficial effects of LLLT on skeletal muscle described by others, including increases in myogenic cell proliferation, gene expression and prevention of local fatigue and muscle damage. The LLLT-induced increase in cytochrome oxidase activity presented here suggests that muscle fibers rapidly respond to photostimulation by enhancing their mitochondrial function, and in particular that of the electron transport chain (32,41). An alternate mechanism of the LLLT-induced increases in muscle cytochrome oxidase activity is a stimulatory effect secondary to nerve terminal stimulation. This is supported by the abundance of mitochondria in the presynaptic compartment of the neuromuscular junction (42), and the high responsiveness of neural tissue to LLLT (30). However, several studies have demonstrated a lack of neuromuscular junction strengthening in response to LLLT (43–45). The present study demonstrated the responsiveness of skeletal muscle to LLLT, but the contributions of neural excitation to this effect cannot be inferred and deserve further investigation.

Despite the positive evidence, skepticism about LLLT still persists because the scientific rationale for *in vivo* treatment protocols is still evolving. It is expected that a better understanding of the effect of variations in biological and LLLT delivery parameters could improve the translational potential of photobiomodulation technologies. The LLLT protocols used in this study were guided by previous studies showing that total cumulative doses of around 20 J cm⁻² can induce increased

cytochrome oxidase activity *in vivo* (20,22,31). Moreover, the middle dose was most effective at increasing cytochrome oxidase activity in the superficial temporalis muscle, followed by the lowest dose, whereas the largest dose induced no significant change compared with the untreated control. These findings are similar to those of a previous study in which we observed that a light dose of 21.6 J cm⁻² given with a similar light source was effective at inducing cytochrome oxidase in the rat, whereas a cumulative dose around 10 J cm⁻² was not (22). The present study corroborates that the specified dosimetric parameters seem to be optimal at inducing metabolic changes in rat tissue. This dose–response effect is characteristic of hormesis. A hormetic dose–response (also known as U-shaped, biphasic or bell-shaped dose–response) consists of stimulation of a biological process at intermediate doses whereas lower and higher doses are less effective. Data presented here supported a hormetic effect of LLLT on skeletal muscle oxidative metabolic capacity such that there was an optimal intermediate light dose that enhanced cytochrome oxidase activity greater than higher and lower light doses. Hormetic models are important because they are superior to linear threshold models in their capacity to accurately predict subtle but biologically meaningful responses below a pharmacological threshold (46). The stimulatory responses to LLLT are usually modest (about 30–60% greater than control values), and contrast with the several-fold increases in a given variable expected according to traditional dose–response models (47). The dose–response phenomenon of hormesis has been observed previously in LLLT applications in muscle, as photostimulatory or photoinhibitory effects have been obtained with low and high energy densities, respectively. For example, using LLLT under *in vitro* conditions in myotube cell cultures, electrical stimulation-induced mitochondrial dysfunction was prevented by low light doses (< 10 J cm⁻²) and was exacerbated by higher doses (11–14 J cm⁻²) (41). Also, lower light doses (4 J cm⁻²) were more effective than larger (8 J cm⁻²) doses at inducing myofibroblast proliferation and reducing inflammation in a model of cutaneous injury (26). Similarly, a relatively low light dose (3.5 J cm⁻²) was more effective than a larger dose (10.5 J cm⁻²) at reducing the myonecrosis and reversing neuromuscular transmission blockade induced by snake venom (28). The effective doses in the above-mentioned studies are notably lower than those in the present study, which could be explained by our *in vivo* transcutaneous and noncontact delivery of LLLT to muscle fibers beneath the scalp's layers (*i.e.* beneath skin, subcutaneous tissue, galea aponeurotica and temporal fascia), all of which contribute to a decrease in the irradiance at the target tissue (48). It has been previously demonstrated that due to the phenomenon of constructive interference, backscattering is particularly high in organs with a solid parenchyma such as muscle, which creates secondary speckling sources within the tissue. This increases the fluence rate by up to 300% at 0.5 mm from the surface. In contrast, at 3 mm the fluence rate is only one-hundredth of that measured at the surface (49). While power densities were not measured at any tissue depth in this study, the induced increase in oxidative metabolic capacity in muscle fibers located well below the muscle surface suggested that energy transmitted through several tissue layers is able to effectively induce metabolic changes in solid organs such as the muscle. Likewise, we have found that with a similar *in vivo* LLLT protocol, light was also able to penetrate to the rat brain

and induce a transcranial increase in cytochrome oxidase activity (22).

Previous studies have demonstrated rapid effects of LLLT on muscle function. For example, LLLT delivered to the humeral biceps muscle immediately before exercise improved the number of contractions by 13%, reduced the latency to contract by 11%, and reduced the serum levels of lactate, creatine kinase and reactive C protein after repeated contractions compared with controls in professional volleyball players (50–54). The changes at 24 h presented here support that induction of cytochrome oxidase activity might be part of the series of early biochemical changes that occur in response to LLLT or other metabolic stimuli and that it might be implicated in modifications of muscle fiber aerobic capacity. Upon elevated energy demands, muscle fibers rapidly engage in a metabolic response that includes increased glucose uptake, mitochondrial biogenesis and increased rate of energy production (55). The earliest reported biochemical change associated with fiber conversion is the increased expression of glucose transporters in the sarcoplasmic membrane that characterizes the red fiber (aerobic) phenotype (56). Such change is detectable as early as 1 h after a single bout of exercise (57,58). White-to-red fiber conversion has been described in response to exercise (59) and other interventions associated with increased intracellular energetic expenditure such as electrical stimulation (60), cross-reinnervation (61), a diet rich in carnitine, carnosine and taurine (62), beta adrenergic stimulation (63), androgen receptor antagonism (64) and mild heat stress (65). However, the results of this study are limited to describing an up-regulation of oxidative capacity as measured by cytochrome oxidase activity. True fiber type conversion can be ultimately defined only through a comparative analysis of myosin heavy chain subtype expression in each fiber. The increases in oxidative capacity and the increases in subsarcolemmal mitochondrial density demonstrated here do not necessarily imply that a complete phenotypic fiber conversion has taken place. The functional relevance of increases in cytochrome oxidase after light therapy should lead to the development of future investigations.

In summary, the present data contribute to the evidence supporting that cytochrome oxidase stimulation with LLLT might represent a noninvasive intervention with potential applications to increase the aerobic potential of skeletal muscle fibers. Cytochrome oxidase might be a candidate target for strategies aimed at boosting mitochondrial function for the development of cytoprotective and performance-enhancing interventions in healthy humans, and at supporting rehabilitation efforts under conditions where muscle contraction and movement are compromised.

Acknowledgements—We thank Frank Lima for building the LED arrays. We also thank Kim Jennings and Jeffrey Conyers for their assistance in delivering low-level light treatment. This study was supported in part by NIH grant MH65728 to Prof. F. Gonzalez-Lima.

REFERENCES

- Alberts, B., A. Johnson, J. Lewis, M. Raff, K. Roberts and P. Walter (2002) Energy conversion: Mitochondria and chloroplasts. In *Molecular Biology of the Cell* (Edited by B. Alberts, A. Johnson, J. Lewis, M. Raff, K. Roberts and P. Walter), pp. 767–829. Garland Science, New York.
- Piccoli, C., R. Scrima, D. Boffoli and N. Capitanio (2006) Control by cytochrome *c* oxidase of the cellular oxidative phosphorylation system depends on the mitochondrial energy state. *Biochem. J.* **396**, 573–583.
- Villani, G. and G. Attardi (1997) In vivo control of respiration by cytochrome *c* oxidase in wild-type and mitochondrial DNA mutation-carrying human cells. *Proc. Natl Acad. Sci. USA* **94**, 1166–1171.
- Kadenbach, B. (2003) Intrinsic and extrinsic uncoupling of oxidative phosphorylation. *Biochim. Biophys. Acta* **1604**, 77–94.
- Dalmonde, M. E., E. Forte, M. L. Genova, A. Giuffrè, P. Sarti and G. Lenaz (2009) Control of respiration by cytochrome *c* oxidase in intact cells: Role of the membrane potential. *J. Biol. Chem.* **284**, 32331–32335.
- Yang, S. J., H. L. Liang and M. T. Wong-Riley (2006) Activity-dependent transcriptional regulation of nuclear respiratory factor-1 in cultured rat visual cortical neurons. *Neuroscience* **141**, 1181–1192.
- Vaynman, S., Z. Ying, A. Wu and F. Gomez-Pinilla (2006) Coupling energy metabolism with a mechanism to support brain-derived neurotrophic factor-mediated synaptic plasticity. *Neuroscience* **139**, 1221–1234.
- Rego, A. C. and C. R. Oliveira (2003) Mitochondrial dysfunction and reactive oxygen species in excitotoxicity and apoptosis: Implications for the pathogenesis of neurodegenerative diseases. *Neurochem. Res.* **28**, 1563–1574.
- Dhar, S. S. and M. T. Wong-Riley (2009) Coupling of energy metabolism and synaptic transmission at the transcriptional level: Role of nuclear respiratory factor 1 in regulating both cytochrome *c* oxidase and NMDA glutamate receptor subunit genes. *J. Neurosci.* **29**, 483–492.
- Wong-Riley, M. T. (1989) Cytochrome oxidase: An endogenous metabolic marker for neuronal activity. *Trends Neurosci.* **12**, 94–101.
- Tanji, K. and E. Bonilla (2007) Optical imaging techniques (histochemical, immunohistochemical, and in situ hybridization staining methods) to visualize mitochondria. *Methods Cell Biol.* **80**, 135–154.
- Pastore, D., M. Greco and S. Passarella (2000) Specific helium-neon laser sensitivity of the purified cytochrome *c* oxidase. *Int. J. Radiat. Biol.* **76**, 863–870.
- Yamanaka, T., Y. Fukumori, M. Numata and T. Yamazaki (1988) The variety of molecular properties of bacterial cytochromes containing heme a. *Ann. N. Y. Acad. Sci.* **550**, 39–46.
- Hamblin, M. R. and T. N. Demidova (2006) Mechanisms of low level light therapy. *Proc. SPIE* **6140**, 1–12.
- Karu, T. (1999) Primary and secondary mechanisms of action of visible to near-IR radiation on cells. *J. Photochem. Photobiol. B, Biol.* **49**, 1–17.
- Wong-Riley, M. T., H. L. Liang, J. T. Eells, B. Chance, M. M. Henry, E. Buchmann, M. Kane and H. T. Whelan (2005) Photobiomodulation directly benefits primary neurons functionally inactivated by toxins: Role of cytochrome *c* oxidase. *J. Biol. Chem.* **280**, 4761–4771.
- Shefer, G., T. A. Partridge, L. Heslop, J. G. Gross, U. Oron and O. Halevy (2002) Low-energy laser irradiation promotes the survival and cell cycle entry of skeletal muscle satellite cells. *J. Cell Sci.* **115**, 1461–1469.
- Zhang, Y., S. Song, C. C. Fong, C. H. Tsang, Z. Yang and M. Yang (2003) cDNA microarray analysis of gene expression profiles in human fibroblast cells irradiated with red light. *J. Invest. Dermatol.* **120**, 849–857.
- Wollman, Y., S. Rochkind and R. Simantov (1996) Low power laser irradiation enhances migration and neurite sprouting of cultured rat embryonal brain cells. *Neurol. Res.* **18**, 467–470.
- Liang, H. L., H. T. Whelan, J. T. Eells, H. Meng, E. Buchmann, A. Lerch-Gaggl and M. Wong-Riley (2006) Photobiomodulation partially rescues visual cortical neurons from cyanide-induced apoptosis. *Neuroscience* **139**, 639–649.
- Wollman, Y. and S. Rochkind (1998) In vitro cellular processes sprouting in cortex microexplants of adult rat brains induced by low power laser irradiation. *Neurol. Res.* **20**, 470–472.

22. Rojas, J. C., J. Lee, J. M. John and F. Gonzalez-Lima (2008) Neuroprotective effects of near-infrared light in an in vivo model of mitochondrial optic neuropathy. *J. Neurosci.* **28**, 13511–13521.
23. Chen, K. H., C. Z. Hong, F. C. Kuo, H. C. Hsu and Y. L. Hsieh (2008) Electrophysiologic effects of a therapeutic laser on myofascial trigger spots of rabbit skeletal muscles. *Am. J. Phys. Med. Rehabil.* **87**, 1006–1014.
24. Lopes-Martins, R. A., R. L. Marcos, P. S. Leonardo, A. C. Prianti Jr, M. N. Muscara, F. Aimbire, L. Frigo, V. V. Iversen and J. M. Bjordal (2006) Effect of low-level laser (Ga-Al-As 655 nm) on skeletal muscle fatigue induced by electrical stimulation in rats. *J. Appl. Physiol.* **101**, 283–288.
25. Iyomasa, D. M., I. Garavelo, M. M. Iyomasa, I. S. Watanabe and J. P. Issa (2009) Ultrastructural analysis of the low level laser therapy effects on the lesioned anterior tibial muscle in the gerbil. *Micron* **40**, 413–418.
26. Medrado, A. R., L. S. Pugliese, S. R. Reis and Z. A. Andrade (2003) Influence of low level laser therapy on wound healing and its biological action upon myofibroblasts. *Lasers Surg. Med.* **32**, 239–244.
27. Rizzi, C. F., J. L. Mauriz, D. S. Freitas Correa, A. J. Moreira, C. G. Zettler, L. I. Filippin, N. P. Marroni and J. Gonzalez-Gallego (2006) Effects of low-level laser therapy (LLLT) on the nuclear factor (NF)-kappaB signaling pathway in traumatized muscle. *Lasers Surg. Med.* **38**, 704–713.
28. Doin-Silva, R., V. Baranauskas, L. Rodrigues-Simioni and M. A. da Cruz-Hoffling (2009) The ability of low level laser therapy to prevent muscle tissue damage induced by snake venom. *Photochem. Photobiol.* **85**, 63–69.
29. Yu, W., J. O. Naim, M. McGowan, K. Ippolito and R. J. Lanzafame (1997) Photomodulation of oxidative metabolism and electron chain enzymes in rat liver mitochondria. *Photochem. Photobiol.* **66**, 866–871.
30. Wong-Riley, M. T., X. Bai, E. Buchmann and H. T. Whelan (2001) Light-emitting diode treatment reverses the effect of TTX on cytochrome oxidase in neurons. *Neuroreport* **12**, 3033–3037.
31. Liang, H. L., H. T. Whelan, J. T. Eells and M. T. Wong-Riley (2008) Near-infrared light via light-emitting diode treatment is therapeutic against rotenone- and 1-methyl-4-phenylpyridinium ion-induced neurotoxicity. *Neuroscience* **153**, 963–974.
32. Silveira, P. C., L. A. Silva, D. B. Fraga, T. P. Freitas, E. L. Streck and R. Pinho (2009) Evaluation of mitochondrial respiratory chain activity in muscle healing by low-level laser therapy. *J. Photochem. Photobiol. B, Biol.* **95**, 89–92.
33. Korfage, J. A. and T. M. Van Eijden (1999) Regional differences in fibre type composition in the human temporalis muscle. *J. Anat.* **194**(Pt 3), 355–362.
34. Tanaka, E., R. Sano, N. Kawai, J. A. Korfage, S. Nakamura, T. Izawa, G. E. Langenbach and K. Tanne (2008) Regional differences in fiber characteristics in the rat temporalis muscle. *J. Anat.* **213**, 743–748.
35. Gonzalez-Lima, F. and A. Cada (1998) Quantitative histochemistry of cytochrome oxidase activity: Theory, methods, and regional brain vulnerability. In *Cytochrome Oxidase in Neuronal Metabolism and Alzheimer's Disease* (Edited by F. Gonzalez-Lima), pp. 55–90. Plenum Press, New York.
36. Gonzalez-Lima, F. and A. Cada (1994) Cytochrome oxidase activity in the auditory system of the mouse: A qualitative and quantitative histochemical study. *Neuroscience* **63**, 559–578.
37. Gundersen, H. J., T. B. Jensen and R. Osterby (1978) Distribution of membrane thickness determined by lineal analysis. *J. Microsc.* **113**, 27–43.
38. Bewick, V., L. Cheek and J. Ball (2004) Statistics review 10: Further nonparametric methods. *Crit. Care* **8**, 196–199.
39. Niemi, K., R. Julkunen-Tiitto, R. Tegelberg and H. Haggman (2005) Light sources with different spectra affect root and mycorrhiza formation in Scots pine in vitro. *Tree Physiol.* **25**, 123–128.
40. Karu, T. (1989) Laser biostimulation: A photobiological phenomenon. *J. Photochem. Photobiol. B, Biol.* **3**, 638–640.
41. Xu, X., X. Zhao, T. C. Liu and H. Pan (2008) Low-intensity laser irradiation improves the mitochondrial dysfunction of C2C12 induced by electrical stimulation. *Photomed. Laser Surg.* **26**, 197–202.
42. Misgeld, T., M. Kerschensteiner, F. M. Bareyre, R. W. Burgess and J. W. Lichtman (2007) Imaging axonal transport of mitochondria in vivo. *Nat. Methods* **4**, 559–561.
43. Comelekoglu, U., S. Bagis, B. Buyukakilli, G. Sahin and C. Erdogan (2002) Electrophysiologic effect of gallium arsenide laser on frog gastrocnemius muscle. *Lasers Surg. Med.* **30**, 221–226.
44. Comelekoglu, U., S. Bagis, B. Buyukakilli, G. Sahin, C. Erdogan and A. Kanik (2002) Acute electrophysiological effect of pulsed gallium-arsenide low-energy laser irradiation on isolated frog sciatic nerve. *Lasers Med. Sci.* **17**, 62–67.
45. Nicolau, R. A., M. S. Martinez, J. Rigau and J. Tomas (2004) Effect of low power 655 nm diode laser irradiation on the neuromuscular junctions of the mouse diaphragm. *Lasers Surg. Med.* **34**, 277–284.
46. Calabrese, E. J. and L. A. Baldwin (2003) Toxicology rethinks its central belief. *Nature* **421**, 691–692.
47. Calabrese, E. J. (2008) Hormesis: Principles and applications for pharmacology and toxicology. *Am. J. Pharmacol. Toxicol.* **3**, 59–71.
48. Ad, N. and U. Oron (2001) Impact of low level laser irradiation on infarct size in the rat following myocardial infarction. *Int. J. Cardiol.* **80**, 109–116.
49. Grimvatov, V., A. Rubinshtein and M. Rubinshtein (2006) Spectral dosimetry in low light therapy. *Proc. SPIE* **6140**, S1–S11.
50. Leal Junior, E. C., R. A. Lopes-Martins, B. M. Baroni, T. De Marchi, R. P. Rossi, D. Grosselli, R. A. Generosi, V. de Godoi, M. Basso, J. L. Mancalossi and J. M. Bjordal (2009) Comparison between single-diode low-level laser therapy (LLLT) and LED multi-diode (cluster) therapy (LEDT) applications before high-intensity exercise. *Photomed. Laser Surg.* **27**, 617–623.
51. Leal Junior, E. C., R. A. Lopes-Martins, B. M. Baroni, T. De Marchi, D. Taufer, D. S. Manfro, M. Rech, V. Danna, D. Grosselli, R. A. Generosi, R. L. Marcos, L. Ramos and J. M. Bjordal (2009) Effect of 830 nm low-level laser therapy applied before high-intensity exercises on skeletal muscle recovery in athletes. *Lasers Med. Sci.* **24**, 857–863.
52. Leal Junior, E. C., R. A. Lopes-Martins, F. Dalan, M. Ferrari, F. M. Sbabo, R. A. Generosi, B. M. Baroni, S. C. Penna, V. V. Iversen and J. M. Bjordal (2008) Effect of 655-nm low-level laser therapy on exercise-induced skeletal muscle fatigue in humans. *Photomed. Laser Surg.* **26**, 419–424.
53. Leal Junior, E. C., R. A. Lopes-Martins, R. P. Rossi, T. De Marchi, B. M. Baroni, V. de Godoi, R. L. Marcos, L. Ramos and J. M. Bjordal (2009) Effect of cluster multi-diode light emitting diode therapy (LEDT) on exercise-induced skeletal muscle fatigue and skeletal muscle recovery in humans. *Lasers Surg. Med.* **41**, 572–577.
54. Leal Junior, E. C., R. A. Lopes-Martins, A. A. Vanin, B. M. Baroni, D. Grosselli, T. De Marchi, V. V. Iversen and J. M. Bjordal (2009) Effect of 830 nm low-level laser therapy in exercise-induced skeletal muscle fatigue in humans. *Lasers Med. Sci.* **24**, 425–431.
55. Holloszy, J. O. (1967) Biochemical adaptations in muscle. Effects of exercise on mitochondrial oxygen uptake and respiratory enzyme activity in skeletal muscle. *J. Biol. Chem.* **242**, 2278–2282.
56. Goodyear, L. J., M. F. Hirshman, R. J. Smith and E. S. Horton (1991) Glucose transporter number, activity, and isoform content in plasma membranes of red and white skeletal muscle. *Am. J. Physiol.* **261**, E556–E561.
57. Booth, F. W. and D. B. Thomason (1991) Molecular and cellular adaptation of muscle in response to exercise: Perspectives of various models. *Physiol. Rev.* **71**, 541–585.
58. Hirshman, M. F., H. Wallberg-Henriksson, L. J. Wardzala, E. D. Horton and E. S. Horton (1988) Acute exercise increases the number of plasma membrane glucose transporters in rat skeletal muscle. *FEBS Lett.* **238**, 235–239.
59. Hayes, A. and D. A. Williams (1996) Beneficial effects of voluntary wheel running on the properties of dystrophic mouse muscle. *J. Appl. Physiol.* **80**, 670–679.
60. Pette, D. (1992) Fiber transformation and fiber replacement in chronically stimulated muscle. *J. Heart Lung Transplant.* **11**, S299–S305.
61. Kikuchi, T., T. Akiba and C. R. Ashmore (1986) Conversion of muscle fiber types in regenerating chicken muscles following cross-reinnervation. *Acta Neuropathol.* **71**, 197–206.

62. Yoshihara, H., J. Wakamatsu, F. Kawabata, S. Mori, A. Haruno, T. Hayashi, T. Sekiguchi, W. Mizunoya, R. Tatsumi, T. Ito and Y. Ikeuchi (2006) Beef extract supplementation increases leg muscle mass and modifies skeletal muscle fiber types in rats. *J. Nutr. Sci. Vitaminol. (Tokyo)* **52**, 183–193.
63. Soic-Vranic, T., D. Bobinac, S. Bajek, R. Jerkovic, D. Malnar-Dragojevic and M. Nikolic (2005) Effect of salbutamol on innervated and denervated rat soleus muscle. *Braz. J. Med. Biol. Res.* **38**, 1799–1805.
64. Ophoff, J., K. Van Proeyen, F. Callewaert, K. De Gendt, K. De Bock, A. Vanden Bosch, G. Verhoeven, P. Hespel and D. Vanderschueren (2009) Androgen signaling in myocytes contributes to the maintenance of muscle mass and fiber type regulation but not to muscle strength or fatigue. *Endocrinology* **150**, 3558–3566.
65. Yamaguchi, T., T. Suzuki, H. Arai, S. Tanabe and Y. Atomi (2010) Continuous mild heat stress induces differentiation of mammalian myoblasts, shifting fiber type from fast to slow. *Am. J. Physiol. Cell Physiol.* **298**, C140–C148.